*Proceedings of the 2012 IEEE 12th International Conference on Bioinformatics & Bioengineering (BIBE), Larnaca, Cyprus, 11-13 November 2012*

# Video Segmentation of the Common Carotid Artery Intima Media Complex

Christos P. Loizou[1], Takis Kasparis[1], Pavlos Papakyriakou[1], Lakis Christodoulou[1], Marios Pantziaris[2], Constandinos S. Pattichis[3]

[1]Departement of Electrical Engineering, Computer Engineering & Informatics, Cyprus University of Technology Limassol, Cyprus, Email: christos.loizou@cut.ac.cy; takis.kasparis@cut.ac.cy; lakis.christodoulou@cut.ac.cy

[2]Institute of Neurology and Genetics, Nicosia Cyprus, mail: pantzari@cing.ac.cy

[3]Department of Computer Science, University of Cyprus, Nicosia, Cyprus, Email: pattichi@cs.ucy.ac.cy

*Abstract*—**The correct identification of the intima-media thickness (IMT) of the common carotid artery (CCA) walls has a high clinical relevance as it represents one of the most reliable predictor for future cardiovascular events. In this work we propose and evaluate an integrated system for the segmentation of the intima-media complex (IMC) and the lumen diameter in longitudinal ultrasound video of the CCA based on normalization, speckle reduction filtering (with a first order statistics filter) and snakes segmentation. The algorithm is initialized in the first video frame of the cardiac cycle by an automated initialization procedure and the borders of the far wall and near wall of the CCA are estimated. The IMC and the carotid diameter are then segmented automatically in the consecutive video frames for one cardiac cycle. The proposed algorithm was evaluated on 10 longitudinal ultrasound B-mode videos of the CCA and is compared with the manual tracings of a neurovascular expert, for every 20 frames in a time span of 3-5 seconds, covering in general 1-2 cardiac cycles. The algorithm estimated an $IMT_{mean}$± standard deviation of (0.72±0.22) mm while the manual results were (0.70±0.19). The mean maximum and minimum diameter was (7.08±1.37) mm and (6.53±1.13) mm respectively. The results were validated based on statistical measures and univariate statistical analysis. It was shown that there was no significant difference between the snakes segmentation measurements and the manual measurements. The proposed integrated system could successfully segment the IMC in ultrasound CCA video sequences thus complementing manual measurements.**

***Keywords-Iintima-media thickness; ultrasound video; carotid artery;***

## I. INTRODUCTION

Cardiovascular diseases (CVD) remain the biggest cause of deaths worldwide, though over the last two decades, cardiovascular mortality rates have declined in many high-income countries. At the same time cardiovascular deaths and disease have increased at an astonishingly fast rate in low- and middle-income countries [1]. The main reason leading to CVD is atherosclerosis, which is the buildup of plaque in the artery walls. The danger is that plaque can lead to aneurysms and blood clots, and clots in turn can result in thrombosis, heart attack, and stroke [1]. Carotid intima-media-thickness (IMT) is a measurement of the thickness of the innermost two layers of the artery wall and provides the distance between the lumen-intima and the media-adventitia interfaces. The IMT can be observed and measured as the double line pattern on both walls of the longitudinal images of the common carotid artery (CCA) [2].

It has been reported that the IMT is a good predictor of stroke incidence [3]. It is also a fact that the increase in the IMT of the CCA is directly associated with an increased risk of myocardial infarction and stroke, especially in elderly adults without any history of cardiovascular disease [1]-[3]. Noninvasive B-mode ultrasound imaging with high resolution is being used to estimate the IMT of the human carotid arteries. Thus, the IMT may be used for the screening of population as at least half of premature heart attacks and strokes, can, and should, be prevented [3]. IMT can be measured through segmentation of the intima media complex (IMC), which corresponds to the intima and media layers (see Fig. 1g and Fig. 1h for the corresponding automated and manual contour segmentations) of the arterial wall. Not only the IMT estimation, but also changes in the mechanical properties of the arterial wall are of interest as, they also have the potential to signalize the existence of early cardiovascular diseases. These changes can be detected by analyzing the arterial wall stiffness (or elasticity) using techniques such as diameter change estimation, artery distensibility or strain imaging [4].

The objective of this work was to investigate a snakes based segmentation method of the IMC in ultrasound imaging of the CCA. This will facilitate the computation of the IMT (of the lower wall) and the artery distensibility characteristics in asymptomatic and symptomatic individuals.

We have found only two studies reported in the literature for segmenting the IMC in ultrasound videos of the CCA. More specifically, in [5] a semi-automatic model based segmentation technique based on the estimated intensity distributions of each CCA image frame was proposed and applied on 30 videos of healthy individuals. In another study [6], a method was developed to measure carotid arterial diameter and IMT from B-mode images that utilizes edge tracking-multiframe image processing that automatically measures arterial diameter and IMT in multiple sequential frames spanning several cardiac cycles. The method was applied to 80 sequential frames of one video. Moreover, diameter and IMT measurements are supported in two

commercial software tools [18], [19]. The later one [19] has FDA approval for clinical use.

There are a number of techniques that have been proposed for the segmentation of the IMC in ultrasound images of the CCA which are discussed in [7]. In two recent studies performed by our group [8], [9] we presented a semi-automatic method for IMC segmentation [8], that incorporated the use of active contours in a normalized rectangular region of interest where speckle removal had been applied [10], [11]. In [9], we presented an extension of the proposed methodology in [8], where also the intima- and adventitia-layers of the CCA could be segmented.

This work presents an automated algorithm for the segmentation and tracking of the IMC and carotid diameter and its distensibility characteristics in ultrasound videos. Following image normalization [10] and despeckle filtering [11], snakes were used to identify an initial intima-lumen boundary for both the near and far walls and thus estimating the diameter change over a cardiac cycle. The resulting segmentation was validated against an expert clinician's manual IMC and diameter segmentation.

## II. Materials & Methods

### A. Recording of Ultrasound Videos

A total of 10 B-mode longitudinal ultrasound videos of the CCA which display the vascular wall as a regular pattern that correlates with anatomical layers were recorded. The videos were acquired by the ATL HDI-5000 ultrasound scanner (Advanced Technology Laboratories, Seattle, USA) [12] with a resolution of 576X768 pixels with 256 gray levels, a spatial gray resolution of 17 pixels per mm (i.e. the resolution is 60μm) and having a frame rate of 100 frames/sec. All video frames were manually resolution-normalized at 16.66 pixels/mm. This was carried out to overcome the small variations in the number of pixels per mm of image depth (i.e for deeply situated carotid arteries, image depth was increased and therefore digital image spatial resolution would have decreased) and in order to maintain uniformity in the digital image spatial resolution [12]. The videos were recorded at the Saint Mary's Hospital, Imperial College of Medicine, Science and Technology, UK, from asymptomatic patients.

### B. Ultrasound Video Normalisation

Brightness adjustments of ultrasound videos were carried out in this study based on the method introduced in [14], which improves image compatibility by reducing the variability introduced by different gain settings, different operators, different equipment, and facilitates ultrasound tissue comparability. Algebraic (linear) scaling of the first video frame was manually performed by linearly adjusting the image so that the median gray level value of the blood was 0-5, and the median gray level of the adventitia (artery wall) was 180-190 [14]. The scale of the gray level of the images ranged from 0-255. Thus the brightness of all pixels in the image was readjusted according to the linear scale defined by selecting the two reference regions. The subsequent frames of the video were then normalized based on the selection of the first frame.

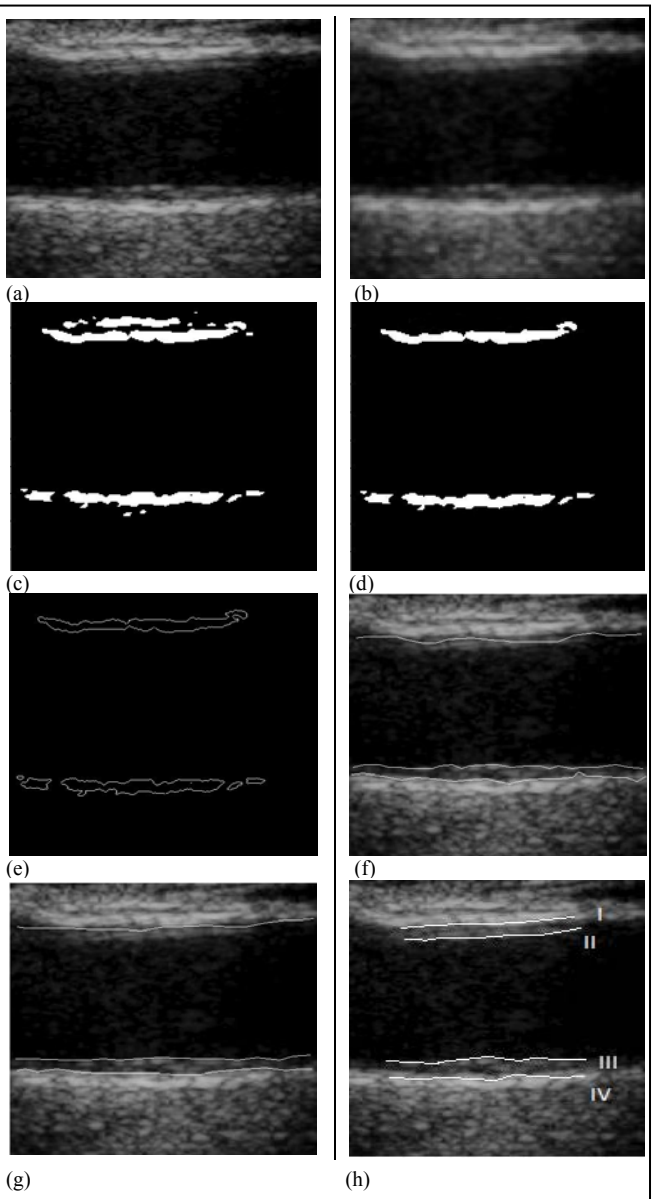


Figure 1. IMT contour initialization procedure and final IMT snakes contour: (a) First frame of the original ultrasound video, (b) Normalised despeckled frame image with DsFhybrimedian filter (2 iterations, window 5x5), (c) binary image frame after dilation with a square window shape of size 9 after removing edges, (d) binary image fraemafter morphology operations, (f) initial snake contours mapped on the first video frame, (g) final snake contour after snakes deformation, (h) manual delineation of IMT with near-wall adventitia (I) and intima (II) and far-wall , intima (III) and adventitia (IV).

### C. Speckle Reduction Filtering (DsFhybridmedian)

In this study the filter DsFhybridmedian, which was introduced in [15] and which produces the median of the outputs generated by median filtering with three different windows (cross shape window, x-shape window and normal window) was applied to each consecutive frame prior to IMC segmentation. The filter was applied twice to each video frame using a 5x5 pixel moving window (see Fig. 1 b).

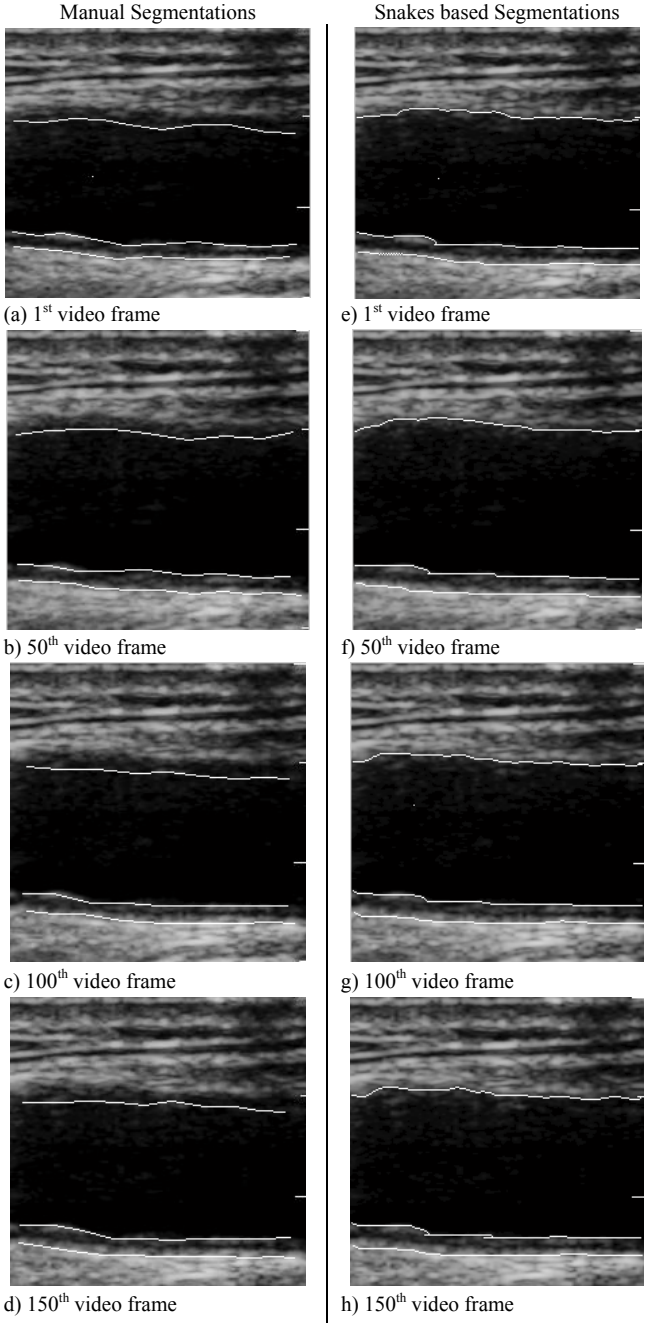


Figure 2. Manual (left column) and automated (right column) video segmenttaion of the CCA for the IMT and carotid diameter, at the a) 1st ($IMT_{man}$=0,85 mm, $diameter_{man}$=6,69 mm, IMT=0,99 mm, diameter=6,9 mm), b) 50th ($IMT_{man}$=0,90 mm, $diameter_{man}$=7,31 mm, IMT=0.93 mm, diameter=7.51 mm), c) 100th ($IMT_{man}$=0,92 mm, $diameter_{man}$=6,98 mm, IMT=0.95 mm, diameter=7.21 mm), and d) 150th ($IMT_{man}$=0,90 mm, $diameter_{man}$=7.11 mm, IMT=0.93 mm, diameter=7.31 mm) video frames of the video (video no. 6 in Table I)

### *D. Manual IMC Segmentation*

An expert (vascular surgeon) manually delineated the IMC borders every 20 frames on 10 longitudinal B-mode ultrasound videos of the CCA. The three contours correspond to the far wall media-adventitia interface, the far wall lumen-intima interface and the near wall intima-lumen interface (see Fig. 1h). This procedure was carried out after image normalization and speckle reduction filtering (see section II.C and section II.D), using MATLAB software developed by our group.

The video segmentations were performed for 3-5 seconds, covering in general 2-3 cardiac cycles, 1cm proximal to the bifurcation of the CCA at a length of 2-3 cm on the far wall. Measurements taken from the near wall are avoided because they are less accurate, caused by overlap of echo pulses, and therefore less reproducible than those taken from the far wall [13]. This is because the adventitia is more echogenic than the blood and bright echoes produced by the adventitia of the near wall can "spill" into the adjacent blood.

### *E. Automated Segmentation Based on Snakes*

The segmentation procedure is described as follows (see Fig. 1): 1) Load the first video frame (see Fig. 1a), perform normalization (in the first frame) (see section II.B) and despeckle filtering (see Section II.C) and apply to all consecutive video frames. The normalized despeckled first video frame is shown in Fig. 1b). 2) Binarize the image by image thresholding, in order to extract edges more easily (see Fig. 1c). 3) Erode the binary image (from point 3) above) by applying an erode morphological operation that eliminates smaller not connected binary image areas (see Fig. 1d). 4) Perform edge detection on the binary eroded image and extract the contoured image (see Fig. 1e). Extract the contour matrix of the above area by locating points and their coordinates on the borders (contours) and construct three interpolating B-splines (The three contours correspond to the far wall media-adventitia interface, the far wall lumen-intima interface and the near wall intima-lumen interface (see Fig. 1h)). Sample the interpolating B-splines in 30 equal segments, in order to define 30 snake elements on the contour. Connect the first and the last snake points on the initial contour to form a closed contour. 5) Map the three detected contours from 4), on the first frame of the video (see Fig. 1f) to form the initial snake contours (see Fig. 1f). 6) Deform the initial contours by the snake to accurately locate the borders and save them (see Fig. 1g). 7) Map the final snake contour from the first video frame, on the second frame of the video, deform by the snake to detect and save the final IMC contours. 8) Repeat the above procedure for all consecutive frames of the video.

The Williams & Shah snakes segmentation method [16] was used to deform the snake and segment the IMC borders. A snake contour may be represented parametrically by $v(s) = [x(s), y(s)]$, where $(x, y) \in \Re^2$ denotes the spatial coordinates of an image, and $s \in [0,1]$ represents the parametric domain. The snake adapts itself by a dynamic process that minimizes an energy function defined as follows [16]:

$$E_{snake}(v(s)) = E_{\text{int}}(v(s)) + E_{image}(v(s)) + E_{external}(v(s)) = \int_s (\alpha(s)E_{cont} + \beta(s)E_{curv} + \gamma(s)E_{image} + E_{external})ds \quad (1)$$

TABLE I. MEAN, MEDIAN, MINIMUM AND MAXIMUM VALUES FOR THE MANUAL AND THEIR CORRESPONDING AUTOMTED IMT DETECTION IN ALL 10 VIDEOS OF THE CCA. THE STANDARD DEVIATIONS ARE GIVEN IN PARENTHESES

| | *MANUAL* | *AUTOMATED* | | | |
|---|---|---|---|---|---|
| *Video* | *Mean(mm)* | *Mean(mm)* | *Median(mm)* | *Min(mm)* | *Max(mm)* |
| 1 | 0.62 (0.17) | 0.64(0.12) | 0.63(0.11) | 0.61 | 0.67(0.09) |
| 2 | 0.68(0.19) | 0.7(0.11) | 0.7(0.10) | 0.63(0.10) | 0.74(0.09) |
| 3 | 0.73(0.22) | 0.73(0.09) | 0.73(0.09) | 0.62(0.11) | 0.78(0.10) |
| 4 | 0.92(0.19) | 0.96(0.10) | 0.97(0.11) | 0.92(0.10) | 1.01(0.11) |
| 5 | 1.11(0.16) | 1.14(0.08) | 1.14(0.11) | 1.1(0.10) | 1.19(0.10) |
| 6 | 0.86(0.21) | 0.87(0.12) | 0.86(0.11) | 0.84(0.10) | 0.91(0.10) |
| 7 | 0.65(0.17) | 0.67(0.12) | 0.67(0.10) | 0.62(0.11) | 0.7(0.11) |
| 8 | 0.47(0.16) | 0.48(0.11) | 0.48(0.12) | 0.45(0.11) | 0.52(0.09) |
| 9 | 0.60(0.17) | 0.61(0.10) | 0.6(0.09) | 0.54(.09) | 0.68(0.09) |
| 10 | 0.40(0.18) | 0.4(0.09) | 0.39(0.09) | 0.36(0.11) | 0.44(0.10) |
| Mean (std) | 0.70 (0.19) | 0.72 (0.22) | 0.71 (0.21) | 0.67 (0.19) | 0.76 (0.21) |
| Min | 0.40 | 0.4 | 1.14 | 1.1 | 0.44 |
| Max | 1.11 | 1.14 | 0.39 | 0.36 | 1.19 |

TABE II. CAROTID DIAMETER DURING CONTRACTION (CDC), CAROTID DIAMETER DURING DISTENSION (CDD), % OF CAROTID WALL DISTENSION (%CWD), MEAN AND MEDIAN DIASTOLIC MEASUREMSNT FOR THE LUMEN DIAMETER IN ALL 10 VIDEOS OF THE CCA . ALL MEASUREMENTS ARE IN MM

| | *MANUAL* | | | *AUTOMATED* | | |
|---|---|---|---|---|---|---|
| *Video* | *CDC* | *CDD* | *%CWD* | *CDC* | *CDD* | *%CWD* |
| 1 | 5.77 | 5.99 | 3.67 | 5.86 | 6.05 | 3.14 |
| 2 | 4.91 | 5.21 | 5.76 | 4.99 | 5.35 | 6.73 |
| 3 | 7.36 | 7.93 | 7.19 | 7.47 | 8.06 | 7.32 |
| 4 | 7.00 | 7.51 | 6.79 | 7.06 | 7.64 | 7.59 |
| 5 | 8.92 | 9.57 | 6.79 | 8.91 | 9.69 | 8.05 |
| 6 | 7.21 | 7.61 | 5.26 | 7.04 | 7.7 | 8.57 |
| 7 | 6.10 | 6.67 | 8.55 | 6.28 | 6.73 | 6.67 |
| 8 | 5.64 | 6,32 | 10.76 | 5.72 | 6.34 | 9.78 |
| 9 | 5.61 | 6.41 | 12.48 | 5.83 | 6.47 | 9.89 |
| 10 | 6.21 | 6.8 | 8.68 | 6.14 | 6.75 | 9.03 |
| Mean (std) | 6.47 (1.16) | 7.0 (1.21) | 7.59 (2.62) | 6.53 (1.1) | 7.08 (1.2) | 7.68 (2.0) |
| Min | 4.91 | 5.21 | 3.67 | 4.99 | 5.35 | 3.14 |
| Max | 8.92 | 9.57 | 12.48 | 8.91 | 9.69 | 9.89 |

*CDC: Carotid diameter during contaction, CDD: Carotid diamete during distension,%CWD: Carotid wall distension*

TABLE III. EVALUATION METRICS BETWEEN THE MANUAL AND THE AUTOMATED IMT SEGMENATATIONS OF THE IMC IN MM

| *Video* | *MAE* | *MARE* | *RMSE* | *NMSE* | *CIMA* |
|---|---|---|---|---|---|
| 1 | 1.89 | 0.024 | 0.297 | 0.088 | 13.54 |
| 2 | 0.54 | 0.013 | 0.135 | 0.018 | 13.37 |
| 3 | 3.17 | 0.075 | 0.503 | 0.253 | 20.31 |
| 4 | 3.15 | 0.050 | 0.370 | 0.150 | 26.07 |
| 5 | 4.41 | 0.070 | 0.499 | 0.249 | 39.00 |
| 6 | 4.68 | 0.082 | 0.534 | 0.285 | 23.56 |
| 7 | 1.62 | 0.037 | 0.368 | 0.135 | 15.68 |
| 8 | 1.21 | 0.067 | 0.596 | 0.356 | 10.38 |
| 9 | 1.62 | 0.037 | 0.368 | 0.135 | 13.67 |
| 10 | 1.21 | 0.067 | 0.597 | 0.356 | 9.09 |
| Mean(std) | 2.35(1.4) | 0.05(0.02) | 0.43(0.14) | 0.20(0.11) | 18.47(9.1) |

*MAE: Mean absolute error, MARE: Mean absolute relative error RMSE: Relative mean square error, NMSE: Normalised mean square error, CIMA: Carotid intima-media area.*

At each iteration step, the energy function is evaluated for the current point in $v(s)$ , and for the points in an $mxn$ neighborhood along the *arc* length $s$ of the contour. Subsequently the point on $v(s)$ is moved to the new position in the neighborhood that gives the minimum energy. The term $E_{\text{int}}(v)$ in (1) denotes the internal energy derived from the physical characteristics of the snake and is given by the continuity $E_{cont}(v)$ and the curvature term $E_{curv}(v)$. It controls the natural behavior of the snake. The internal energy contains a first-order derivative controlled by $\alpha(s)$, which discourages stretching and makes the model behave like an elastic string by introducing tension and a second order term controlled by $\beta(s)$, which discourages bending and makes the model behave like a rigid rod by producing stiffness. The weighting parameters $\alpha(s)$ and $\beta(s)$ can be used to control the strength of the model's tension and stiffness, respectively. Altering the parameters $\alpha, \beta$ and $\gamma$ may control the operation of the snake. The second term in (1) $E_{image}(v)$, represents the image energy due to some relevant features such as the gradient of edges, lines, regions and texture [16]. It attracts the snake to low-level features such as brightness and edge data. Finally, the term $E_{external}(v)$ is the external energy of the snake, that is user defined and is optional.

The method was also proposed and evaluated in [8] and [9], in 100 ultrasound images of the CCA and more details about the model can be found there. For the Williams & Shah snake, the strength, tension and stiffness parameters were equal to $\alpha_s = 0.6$, $\beta_s = 0.4$, and $\gamma_s = 2$ respectively.

### *F. Measurements*

Measurements were carried out for 3-5 seconds, covering in general 2-3 cardiac cycles, 1cm proximal to the bifurcation. The manual IMT was measured in the first frame and then every 20 frames per subject over the whole cardiac cycle. The automated IMT was measured at each frame per subject over the whole cardiac cycle. The distance was computed between the two boundaries, at all points along the arterial segment of interest moving perpendicularly between pixel pairs, and then averaged to obtain the mean IMT ($IMT_{mean}$). Also the maximum ($IMT_{max}$), minimum ($IMT_{min}$), and median ($IMT_{median}$) IMT values, are calculated. Figure 1g shows the detected $IMT_{mean}$ on the first video frame (see also Fig. 2a)-d) for IMC detection on different video frames).

In order to investigate how the results of the snakes segmentation method differ from the manual delineation results, we used the following measurements. We computed the parameters $IMT_{mean}$, $IMT_{min}$, $IMT_{max}$, and $IMT_{median}$, for each video frame as well as the standard deviation over the whole video frames at end diastole. We have also computed the carotid diameter during contraction (CDC), the carotid diameter during distension (CDD) and the percentage of the carotid wall distension (%CWD=((CDD-CDC)/CDC)*100%).

### *G. Evaluation Metrics*

Furthermore, in order to evaluate our algorithm, the following evaluation metrics between the automated and manual contours for all three detected borders were computed.

The three contours correspond to the far wall media-adventitia interface, the far wall lumen-intima interface and the near wall intima-lumen interface (see Fig. 1h).

*1) The mean average error (MAE):*

$$MAE = \sum_i |A_i - M_i| / N$$

*2) The mean average randomized error:*

$$MARE = \sum_i \left| \frac{A_i - M_i}{M_i} \right| / N \cdot$$

*3) The randomized mean square error (RMSE):*

$$RMSE = \sqrt{\sum_i |A_i - M_i|^2} / (N)$$

where A and M represent the automated and manual contour points and N is the number of points.

*4) The normalized mean square error (NMSE):*

$$NMSE = 100 * RMSE / std_N$$

with $std_N$ is the standard deviation over all timings.

*5) The carotid intima-media area (CIMA):*

$$CIMA = \pi * (0.5 * CDC + IMT)^2 - \pi * (0.5CDC)^2$$

## III. RESULTS

Figure 2 illustrates an example of a CCA video IMT and carotid diameter manual (see Fig. 2, left column) and automated (see Fig. 2, right column) segmentations at, the 1st, 50th, 100th and 150th frames of video. It shown, that manual and automated segmentation measurements are visually very similar. Figure 3a illustrates the lumen rate of change of a video of a CCA, showing the diameter change over all video frames, while Fig. 3b presents the IMT rate of change over all video frames for one cardiac cycle. It is shown that the IMT has a variation of 0.02 mm over all cardiac cycles, with a mean IMT of 0.84mm, while the diameter ranges between 6.9 mm and 7.63mm, with a carotid diameter difference of 0.73mm. Table I illustrates the results for the mean, median, minimum and maximum IMT values estimated manually and automatically from the proposed algorithm for all videos investigated. The results after the automated segmentation of all 10 videos of the CCA gave values of $IMT_{mean}$=0.72±0.4mm, $IMT_{medain}$=0.71±0.21mm, $IMT_{min}$=0.67±1.1mm, $IMT_{mean}$=0.76±0.21mm. No significance difference was found between the manual and the automated IMT segmentation measurements (p=0.003). Table II presents the manual and automated results of the carotid diameter during contraction (CDC), the carotid diameter during distension (CDD) (CDC=6.53±1.1mm, CDD=7.08±1.2mm) and the percentage of the carotid wall distension (%CWD=((CDD-CDC)/CDC)*100%), which was %CWD=7.67±1.9. We found significant differences between the manual and the automated CDC and %CWD ((p=0.13 and p=0.92) and no significant differences for the CDD (p=0.006). Table III presents the results of the evaluation metrics between the manual and the automated delineations of the IMT (average(std)) in millimeters, for all 10 videos of the CCA with RMSE=0.43±0.14mm, MSE=0.20±0.11, MAE=2.35±1.4, and MARE=0.05±0.02 respectively

## IV. DISCUSSION

The results of the proposed semi automatic IMC and diameter video segmentation method can be favorably compared to the results of the segmentation of the carotid plaque in ultrasound images presented in our recent studies [8], [9], and also with the results presented in [5], [6] and [17]. Comparing the proposed video segmentation technique with our previous study in [8] and [9], where segmentation of 100 images were of the CCA were performed ($IMT_{mean}$=0.69±0.13mm) we may observe that values of the IMT estimated in this study are larger ($IMT_{mean}$=0.72±0.22mm) and with higher standard deviation. The higher standard deviation is due to the fact that the snake contour will not be so accurately repositioned in the following frames and converges to a different location. The average computation of the snake contour was about 15 seconds per frame. Taking into account that the expert clinician required over 25 seconds per frame for the manual delineation and the fact that there are about 500 frames per cardiac cycle, there is an average time saving of 8 minutes per video assuming manual segmentation is carried out every 20 frames. It should also be noted that the accuracy of the method may be improved if the first frame snake initialization is more accurate. The results of this study showed that the automated measurements are highly reproducible (see Tables I-III) where the proposed method over estimates the IMT and diameter with a small error of about 0.015.

In [5] and [6] images were neither normalized nor despeckled nor an automatic contour estimation was used as in this study. The normalization used in this study ensures that the method and the results are not dependent on the equipment used. This is not the case for the video segmentation method

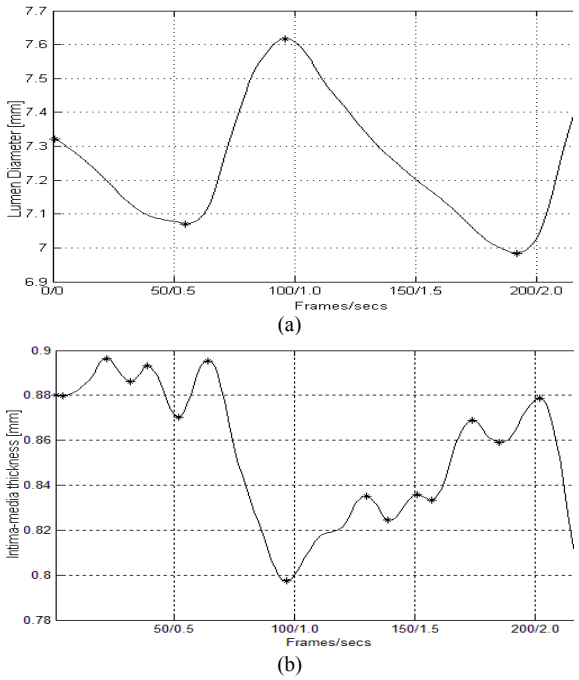


Figure 3. Lumen rate of change for the video of Fig.2, showing in a) the diameter change over two cardiac cycles, and in b) the IMT rate of change for one cardiac cycle.

proposed in [5], where the region based segmentation was established using the statistical distribution of the gray level of the frames whilst speckle noise was not taken into consideration. The method is fast and does not require extensive user interaction. The evaluation of the method results in a mean of IMT difference of 0.02 mm with a standard deviation of 0.19 mm and compares favorably to other automated methods presented in the literature [5], [6]. A commercialized software system [18] for longitudinal image and video segmentation, which also supports DICOM image analysis of the IMT is available, where diameter and IMT changes over the cardiac cycle can be measured. Finally, in [20], a software tool based on snakes for efficient semi-automated annotation of images and image sequences was presented. Further improvement could be achieved to enable the use of the proposed video segmentation technique in the real clinical praxis if the initialization of the snake contours (see Section II.E) is applied every 30 or 40 frames so that the snake contour is repositioned closer to the plaque borders. Additionally, the longitudinal movement and the resulting shear strain of the CCA may be investigated as in [21], where similar findings for the IMT and diameter rate of change were found. Furthermore, the neighboring frames correlation may be utilized in order to achieve a more robust method. It seems that the assistance of humans will remain essential in any practical image and video segmentation method, therefore incorporating high-level human knowledge algorithmically into the computer still remains a challenge. With a large number of segmentation algorithms being developed in last few years the performance evaluation of these algorithms will also attract more research efforts. The results of this study show very good agreement with the expert clinician's segmentation, though an evaluation on a larger dataset will take place.

## V. Concluding Remarks

This paper presents a fully automated method for the segmentation of the IMC so that the IMT can be evaluated. The IMC in the near wall of the CCA is not properly detected due to the nature of US imaging, thus the segmentation algorithm is developed for segmentation of the IMC at the far wall, where the borders are visible [6]. The success of the algorithm is due to the use of the available anatomical information regarding the position and general structure of the CCA to establish the best possible outcome. The algorithm is evaluated on images from 10 cases with a mean IMT difference of 0.09 mm. The algorithm works well even on difficult cases, but further evaluation is required. Future work will involve assessment of the algorithm on a much larger dataset and discussion of how inter- and intra-observer variability affects the evaluation of the results.

## Acknowledgment

This work was partially funded by the Cyprus University of Technology under the contract named TILEPISKOPISI.

## References

[1] S. Mendis, P. Puska, B. Norrving, (Ed.), Global Atlas on cardiovascular disease prevention and control, Geneva: World Heart Organization, 2011. ISBN 978-92-4-156437-3.

[2] P. Touboul, M. Hennerici, S. Meairs, H. Adams, P. Amarenco *et al*., "Mannheim carotid intima-media thickness consensus (2004–2006)," *Cerebrovascular Diseases*, vol. 23, pp. 75–80, 2007.

[3] I. M. van der Meer, M. L. Bots, A. Hofman, *et al*., "Predictive value of noninvasive measures of atherosclerosis for incident myocardial infarction: the Rotterdam Study," *Circulation*, vol. 109, no. 9, pp. 1089–94, 2004.

[4] M. Cinthio, A. R. Ahlgren, T. Jansson, A. Eriksson, H. W. Persson, and K. Lindstrom, "Evaluation of an ultrasonic echo-tracking method for measurements of arterial wall movements in two dimensions", *IEEE Trans. Ultr. Fer. Freq. Contr.*, vol. 52, no. 8, pp. 1300-1311, Aug. 2005.

[5] F. Destrempes, J. Meunier, M. F. Giroux, G. Soulez, and G. Cloutier, "Segmentation in ultrasonic Bmode images of healthy carotid arteries using mixtures of Nakagami distributions and stochastic optimization", *IEEE Trans. Med. Imag.*, vol. 28, no. 2, pp. 215-29, February 2009.

[6] R.H. Selzer, W.J. Mack, P.L. Lee, H. Wwong-Fu, *et al*., "Improved common carotid elasticity and intima-media thickness measuremnts from computer analysis of sequential ultrasound frames," *Atherosclerosis*, vol. 154, pp. 185-193, 2011.

[7] F. Molinari, G. Zeng, and J. S. Suri, "A state of the art review on intima-media thickness measurement and wall segmentation techniques for carotid ultrasound," *Comp. Meth. Progr. Biomed.* , vol. 100, pp. 201 – 221, 2010.

[8] C.P. Loizou, C. Pattichis, M. Pantziaris, T. Tyllis, and A. Nicolaides, "Snakes based segmentation of the common carotid artery intima media," *Med. Biolog. Eng. Comput.,* vol. 45, pp. 35–49, 2007.

[9] C.P. Loizou, C.S. Pattichis, A. Nicolaides, M. Pantziaris, "Manual and automated media and intima thickness measurements of the common carotid artery," *IEEE Trans. Ultr. Fer. Freq. Contr.,* vol. 56, no. 5, pp. 983-994, May 2009.

[10] C.P. Loizou and C.S. Pattichis, "Despeckle filtering algorithms and Software for Ultrasound Imaging", Synthesis Lectures on Algorithms and Software for Engineering, Ed. Morgan & Claypool Publishers, 1537 Fourth Street, Suite 228, San Rafael, CA 94901 USA, June 2008, ISBN-13: 9781598296204.

[11] C.P. Loizou, C.S. Pattichis, *et al*., "Comparative evaluation of despeckle filtering in ultrasound imaging of the carotid artery," IEEE Trans. Ultras. Ferroel. Freq. Contr., vol. 52, no. 10, pp. 1653-1669, 2005.

[12] A Philips Medical System Company, "Comparison of image clarity, SonoCT real-time compound imaging versus conventional 2D ultrasound imaging," ATL Ultrasound, Report, 2001.

[13] P. Pignoli, E. Tremoli, A. Poli, P. Oreste, and R. Paoletti, "Intima plus media thickness of the arterial wall: A direct measurement with ultrasound imaging," *Atheroscler*., vol. 74, no. 6, pp. 1399-1406, 1986.

[14] T. Elatrozy, A. Nicolaides, T. Tegos, A. Zarka, M. Griffin, and M. Sabetai, "The effect of B-mode ultrasonic image standardization of the echodensity of symptomatic and asymptomatic carotid bifurcation plaque," *Int. Angiol.,* vol. 17, no. 3, pp. 179-186, 1998.

[15] A. Nieminen, P. Heinonen, and Y. Neuvo, "A new class of detail-preserving filters for image processing*", IEEE Trans. Pattern Anal. Mach. Intell.*, vol. 9, pp. 74-90, 1987.

[16] D. J. Williams and M. Shah, "A fast algorithm for active contours and curvature estimation," *Int. J. on Graph.,, Vision and Imag. Proc.: Image Underst.*, vol. 55, pp. 14 – 26, 1992.

[17] C.P. Loizou, M. Pantziaris, C.S. Pattichis, E. Kyriakou, "M-mode state-based identification in ultrasound videos of the common carotid artery," *Proc. 4th Int. Symp. Commun. Contr. Sign. Proces., ISCCSP 2010*, Limassol, Cyprus, pages 6, March 3-5, 2010.

[18] Esaote North America Inc., 8000 Casteway Drive, Indianapolis, IN 46250, USA. http://www.esaote.com

[19] Medical Imaging Applications LLC, Coralville, Iowa 52241, USA. http://www.mia-llc.com/

[20] D.K. Iakovidis, C.V Smailis, "Efficient Semantically-Aware Annotation of Images", *Proc. IEEE Int. Conf. Imag. Systems and Techniques (IST)*, pp. 146-149, Penang, Malaysia, May 2011.

[21] M. Cinthio, A..R. Ahlgren, J. Bergvist, T. Jansson, *et al*., "Longitudinal movenets and resulting shear strain of the arterial wall", *Am J. Heart Circ. Physiol*., vol. 291, pp. 394-402, 2005.